Universiteit
Leiden
The Netherlands

Probing quantum puddles: nonlinear dynamics in superfluid film optomechanics

Raabe, L.D.

Citation
Raabe, L. D. (2026, September 8). *Probing quantum puddles: nonlinear dynamics in superfluid film optomechanics*. Retrieved from https://hdl.handle.net/1887/4309261

Version:	Publisher's Version
License:	Licence agreement concerning inclusion of doctoral thesis in the Institutional Repository of the University of Leiden
Downloaded from:	https://hdl.handle.net/1887/4309261

Note: To cite this publication please use the final published version (if applicable).

Chapter 4

Optical ring resonators at mK temperatures

In this chapter, we present our experimental platform to cool a tapered fiber-resonator setup to mK temperatures and the control algorithm for cryogenic stepper motors that actively preserves the alignment of the tapered fiber and optical resonator while cooling down. The optical setup fits into a superfluid tight enclosure. Furthermore, the fabrication process for tapered optical fibers is described.

4.1 Introduction

Microfabricated ring resonators have been used in a large variety of studies reaching from cavity optomechanics and quantum optics to nonlinear optics [42, 77]. These devices can be quickly improved and iterated upon due to the compatibility with semiconductor processing techniques. Cooling these devices to mK temperatures enables a variety of improvements, such as lower noise [78], longer coherence of embedded ions [46, 79], or the possibility of cavity optomechanics experiments with thin films of superfluid helium condensed on the optical resonator surface [25, 26]. However, differing thermal expansion coefficients among the systems components pose challenges in maintaining optical alignment during cooldown. Solutions to maintain optical alignment reach from glued packaging [80] to self-aligning systems [81]. The use of cryogenic stepper motors enables continued adjustment of the optical alignment [82], but manual continuous realignment over the typical cooldown time of multiple days is undesirable and challenging without optical access to the setup.

4.2 Room temperature preparation and measurements

Low-temperature experiments with optical ring resonators require careful preparation and characterization at room temperature. After fabricating a tapered fiber, we measure quality factors (Q-factor) of the selected sample and characterize the transmission over 1 FSR to adjust parameters of our control algorithm to the experimental system.

4.2.1 Fiber Taper

Tapered fibers are a relatively quick and reproducible way to couple light to resonant structures such as wedge resonators or torroids. They combine adjustable evanescent coupling with the ability to adiabatically shape the optical mode to match different device geometries by tuning the length of the taper [43] (see chapter 2).

We developed and built a setup to reliably produce high-quality tapered optical fibers from commercially available optical fiber, based on a similar setup of the Vahala group at Caltech. The setup consists of a ceramic microheater and a stage with two motorized actuators that allow the fiber to be pulled evenly away from the heated area. Two springs and a manual actuator are integrated into the stage to allow adjustment to

the tension of the fiber after pulling. To produce a tapered fiber, we first prepare the fiber by removing 30 to 40 mm of the coating in the middle of the fiber and cleaning the area with isopropanol. The fiber is then placed into two grooves and secured with rubber clamps, such that the cleaned region lies between the clamps. We heat the ceramic micro heater slowly to a temperature of about 1500 °C far away from the fiber, before we lower it onto the fiber. We place the heater such that the fiber sits in the hottest region but does not touch the walls of the heater. We then wait for the fiber to thermalize for 60 seconds. Afterwards, we start the pulling process by using the motorized stages to evenly pull both clamps away from the heater with a velocity of 20 μm/s until the fiber has extended by 24 mm to 36 mm. The heater is then slowly retracted and ramped down. This step should not be sped up because thermal shocks can significantly reduce the transmission of the tapered regions. However, leaving the tapered fiber too long in the heater causes further elongation and sagging of the fiber. The most consistent results were achieved when retracting the heater over a time span of 20-30 seconds. Almost the entire tapering process is computer controlled, needing only manual intervention for the preparation of the fiber and the horizontal positioning of the heater.

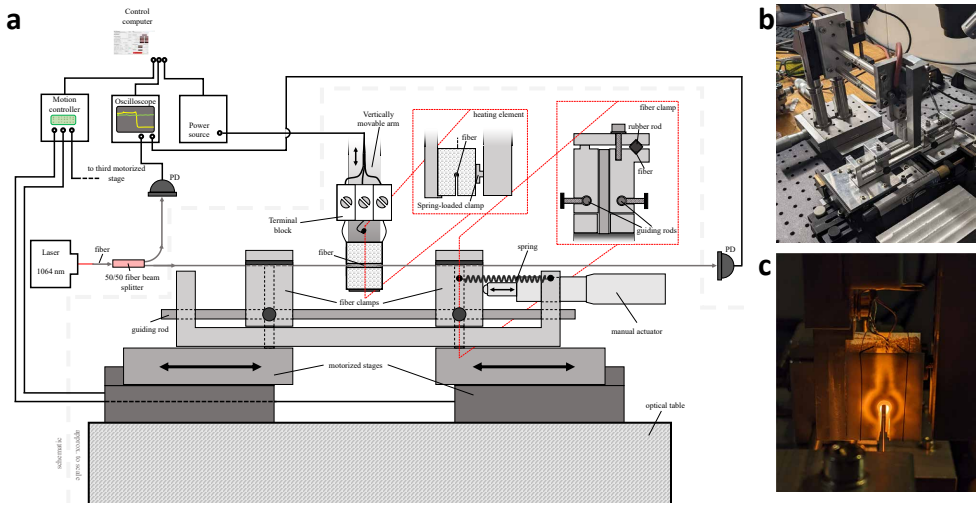

Figure 4.1: Fiber taper setup. **(a)** Schematic of the setup to produce tapered fibers (adapted from [83]). **(b)** Picture of the setup to produce tapered fibers as built in our lab. **(c)** Picture of the ceramic micro-heater at 1500 °C and an inserted fiber during the fiber tapering process.

While we produce the tapered optical fiber, we continuously monitor its transmis-

sion at different frequencies. The transmission typically shows a sinusoid fluctuation with an increasing frequency over time during the extension of the fiber. This stems from interference with additional reflections in the system. This interference pattern disappears as soon as the tapering process is finished, but should be taken into account when comparing the transmission. Often the tapered fiber is not fully under tension once the heater has been retracted, leading to additional bending losses. This can be rectified by carefully adjusting the tension on the fiber using the manual actuator. Generally, with increasing tension the bending losses will slowly decrease until maximum transmission is reached. Small further increases in tension lead to strain losses before the fiber breaks, which enables careful tuning of the tension for maximum transmission. Using this method, we have been able to consistently produce tapered fibers with a length of 24 to 30 mm and a transmission of over 90% across a scanning range of several GHz. This enables us to evanescently couple to a range of device sizes and shapes. We have achieved critical coupling to 6 mm diameter wedge resonators as well as 50 μm diameter toroidal microresonators and up to 80% coupling to 12 μm spheres (see figure 4.2).

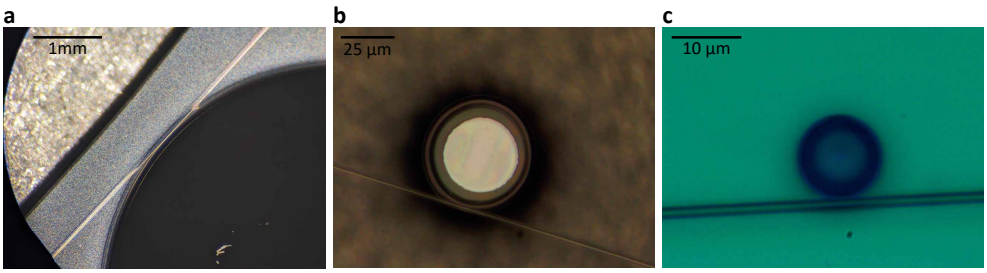

Figure 4.2: Optical coupling to different devices using a tapered fiber. **(a)** Fiber position for critical coupling to a 6 mm diameter wedge resonator. **(b)** Fiber position for critical coupling to a toroid microresonator. **(c)** Fiber position for 80% coupling to a microsphere resonator. All scale bars are approximate.

4.2.2 System characterization

To couple light into an optical ring resonator, we place the tapered fiber under a microscope and add the optical resonator on a 3-axis translation stage. We monitor transmission through the fiber while the input laser is slowly scanned over more than one free spectral range (FSR). We then roughly align the center of the tapered fiber with the edge of the resonator and put the fiber into the focus of the microscope. We

slowly move the optical resonator upwards towards the fiber until the resonator starts coming into focus. We then realign the edge of the optical resonator to the center of the tapered fiber under the microscope and move the optical resonator further up. We repeat the previous two steps until evanescent coupling, indicated by dips in transmission, is achieved.

Generally, there are 3 coupling regimes as the tapered fiber moves closer to the resonator with a radius r: undercoupling, critical coupling and overcoupling. In the undercoupling regime a part of the light is coupled into the resonator and leads to destructive interference in transmission if the resonance condition $\lambda = 2\pi r$ is met. This regime is generally reached if the fiber is far away from the resonator, resulting in only part of the evanescent field to couple into the device. When moving closer to the resonator the coupling increases until the field coupled out of the resonator and the field in the fiber perfectly destructively interfere. This is the point of critical coupling. At this point there is mode matching between the fiber mode and the resonator mode. Therefore, the exact spatial point of critical coupling depends on the exact geometry of the resonator. If a taper is pulled too thick compared to the mode size of the device, a perfect mode-match is not possible and therefore no critical coupling. Moving the fiber through the critical coupling point closer to the resonator leads to overcoupling. At this point the free space between fiber and resonator becomes small enough to weakly confine light, creating an additional cavity with low optical Q-factor. This leads to additional interference effects leading to spectrally broad depressions in the off-resonance transmission. At the same time, the modes in fiber and resonator start to be mismatched again, leading to only partial destructive interference. These effects increase until the fiber touches the resonator.

For the experiments presented in this thesis, we use an optical wedge ring resonator with a radius of 3 mm and an undercut of about 100 μm. For this device, coupling to optical resonator modes is possible at the edge of the optical resonator in a region of about 100 μm parallel to the resonator surface and 10 μm in height (see figure 4.3). Because of the large size of these devices, they support many modes, making it generally difficult to reliably identify the fundamental mode[1] (see figure 3.2(a)). However, lower order modes tend to feature a higher quality factor, making some distinction possible. Placing the fiber over the bulk of the resonator leads to absorption proportional to

[1] The fundamental mode has a Gaussian intensity profile in the transverse direction. In general, it has the highest optical quality factor of any mode supported by the device.

the length of the fiber that touches the resonator. As the fiber is moved over the undercut, we observe overcoupling and absorption if the fiber touches the resonator. Moving the fiber closer to the edge reduces the absorption and allows us to increase coupling. When the fiber is close to the edge, moving the fiber down allows to transition between the undercoupling and overcoupling regimes. The transition happens abruptly, because electrostatic forces pull the fiber to the optical resonator once it is close enough. At this point, we are able to observe a very dense distribution of modes. Only if the fiber is placed to exactly overlap with the outer edge of the resonator is it possible to move smoothly between undercoupling, critical coupling and overcoupling. Additionally, we couple to only a few modes. Considering the mode shape in the fiber and the position of the fundamental mode of the optical resonator, at this point it is likely that the mode with the highest Q-factor and critical coupling is the fundamental mode.

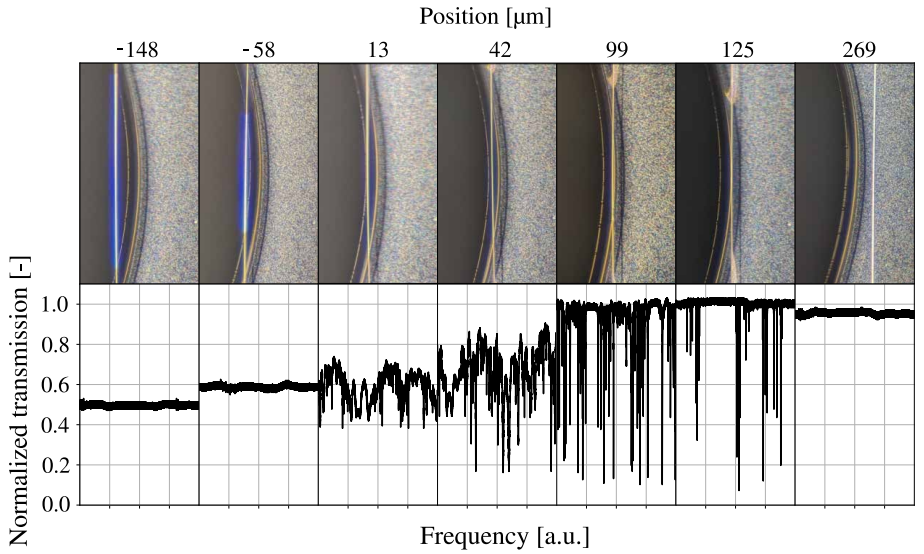

Figure 4.3: Transmission at different optical alignments. Fiber positions and the corresponding transmission spectra. Above the bulk resonator there is only absorption leading to reduced transmission. As the fiber is moved towards the undercut we transition from the overcoupling regime closer to critical coupling. Adapted from [83].

4.3 Cooldown

Cooling an optical setup that is sensitive to misalignment of a few μm to 4 K and below comes with a set of challenges due to thermal expansion of the different components [84]. Our dilution refrigerator takes a few days to cool from room temperature to 4 K, which makes active monitoring inconvenient. Since we also do not have direct optical access to our experiment we can only rely on transmission measurements to determine the state of optical alignment. These constraints made it necessary to implement active computer-controlled feedback and optical realignment.

4.3.1 Packaging

Early cooldown tests showed that simply aligning the tapered fiber to the large wedge resonator and gluing the setup to an Invar holder leads to misalignment of the components while cooling down. Mismatched thermal expansion coefficients between the sample, the Invar block and the glue lead to an effective downward motion of the fiber. As the fiber touches the resonator edge, strain between the two components builds up, leading either to the fiber suddenly slipping underneath the undercut far away from the coupling region or the fiber breaking.

To counteract this misalignment we mount the fiber and sample on two cryogenic stepper motors, allowing us to move the optical ring resonator vertically and the fiber horizontally, perpendicular to its elongation. Movement in the two directions was separated to avoid crosstalk. Small positioning changes along the fiber do not lead to differences in coupling behavior and therefore do not need to be compensated. The optical ring resonator is placed on a horizontal sample holder and secured by a small drop of vacuum grease to keep the sample in place, but make rapid sample exchange possible. The sample holder is attached directly to the vertical stepper motor. We developed a light-weight holder for the tapered fiber made of Invar to minimize changes in tension of the tapered fiber. The holder features two inner gluing points with grooves to ensure the fiber is mounted exactly straight and two outer gluing points that act as strain relief.

To glue the tapered fiber onto the low-temperature (LT) fiber holder, the fiber is initially left in the rubber clamps described above. This is done to minimize the risk of the fiber breaking and to maintain steady tension. We mount the LT fiber holder on a manual translation stage, align the fiber to the grooves of the LT fiber holder

and slowly approach the fiber from below. Once the setup is nicely aligned, we pull the LT fiber holder back and attach a very small amount of Stycast[2] with the tip of a syringe to the outermost position of the inner gluing points. Then we add a larger drop of Stycast to the outer gluing points. The LT fiber holder is then slowly returned to the pre-aligned position, while monitoring the transmission through the fiber and verifying that the fiber is covered by Stycast at all four mounting points through a microscope (see figure 4.4). If the fiber is not covered at the outer gluing points, it is possible to add an additional drop of Stycast, while the LT fiber holder is aligned with the fiber. If the fiber is not covered at the inner gluing points, we recommend pulling the fiber holder back, adding a small amount of glue and restarting the process described above. Once the setup is nicely aligned, we let the glue cure for at least 12 hours, before opening the rubber clamps and mounting the LT fiber holder. We have found that long tapers with a size of 15 mm or above experience a large losses once the fiber touches the Stycast at the inner mounting points. This may be caused by the fiber already supporting an evanescent field outside the fiber at the inner gluing points. For coupling to smaller devices, thinner and longer fiber tapers are needed, due to the decreased mode volume in the smaller device. We therefore recommend making an additional LT fiber holder with increased distance between the inner mounting points for experiments with small devices.

The LT fiber holder is mounted directly onto the horizontal stepper motor. We emphasized this part to be light-weight because we wanted to avoid imbalance and failure of the stepper motor due to the holder having a significant overhang. Both motors are attached to a copper frame through mounting plates. The entire optical setup, which we refer to as 'boat', is designed to fit into the superfluid cell, a copper tube with an inner diameter of 60 mm (see figure 4.5 (a)). The tube can be sealed with two lids with 24 screws each and indium wires to make it superfluid tight. The two lids feature feedthroughs for fibers and wires as well as a capillary to control the amount of helium inside the cell.

We assemble the boat by first attaching the fiber and its positioner to the copper frame. We then make sure that the sample positioner is in its lowest position and carefully place the copper frame over the sample holder. Once the sample holder is in position, we carefully attach it to the boat to complete the assembly. The entire process is shown in figure 4.4. Placing the boat under a microscope allows us to find

[2]Loctite Stycast 2850 FT with Catalyst 24LV

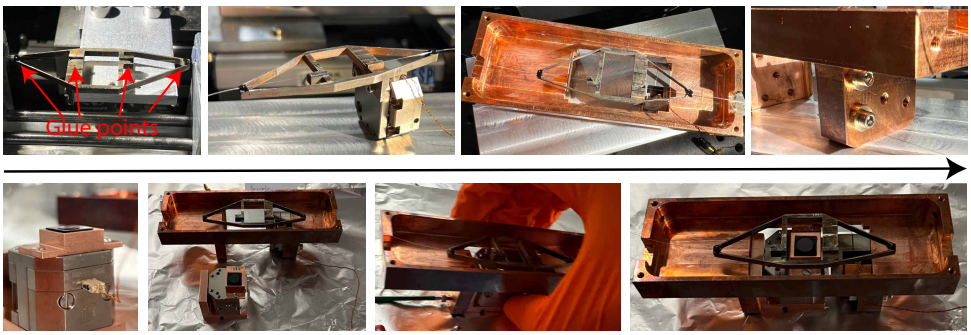

Figure 4.4: Process of assembling the optical setup. Pictures showing the various steps to assemble the optical setup. From left to right and top to bottom. The fiber is glued on the fiber holder which is mounted on a stepper motor. The assembly is mounted in the holder. The optical ring resonator and holder is mounted on a second stepper motor and mounted on the holder.

optical coupling by moving the positioners as described above. We generally place the fiber at a position at which it attaches to the resonator, but we do not see a large amount of overcoupling. The aligned assembly is slid into the superfluid cell and attached to the top of it. We then splice the fiber taper to the feedthrough fibers and connect the motors to the feedthrough wires. After checking that the optical coupling is maintained, we close and seal the first lid using an Indium seal. The entire assembly is then transported to our dilution refrigerator and attached to a vibration isolation stage hanging from the bottom of the mixing chamber (see figure 4.5 (b), (c)). We then close and seal the second lid featuring the capillary feedthrough.

4.3.2 Keeping coupling while cooling down

In principle, it would be possible to retract the sample and sweep the range of the motors once the setup has been cooled down to 4 K. However, we found that the fragile taper breaks quite easily during such a sweep. Instead, we utilize the characterization of coupling described above to develop a control algorithm that keeps coupling to the ring resonator while cooling to 4 K. From there we can easily optimize the coupling to the desired mode.

While cooling down we scan the laser over more than 1 FSR and measure the transmission through the fiber. The control algorithm works as follows. We define the average of the off-resonant transmission as a base value B. For the fiber to have no coupling,

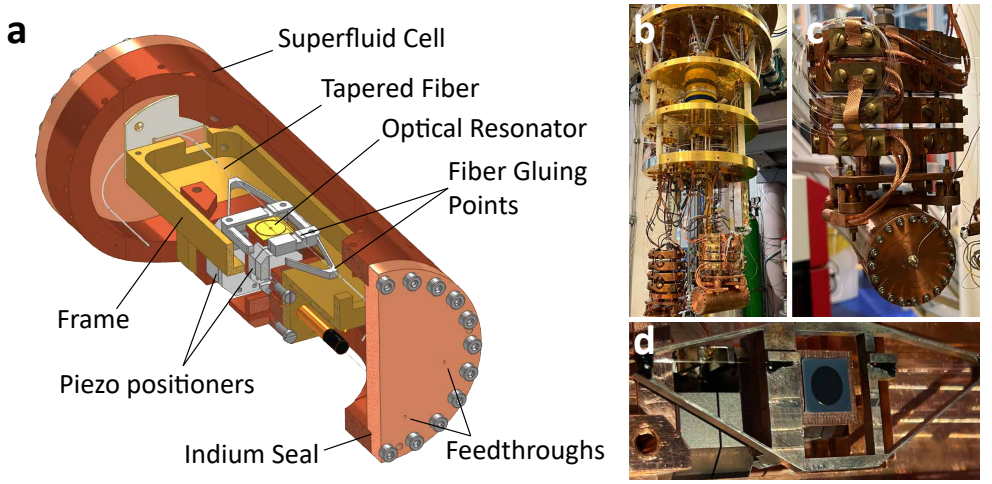

Figure 4.5: Experimental setup for superfluid optomechanics experiments. **(a)** Schematic of the optical setup inside a superfluid tight container. **(b),(c)** Pictures of the experimental setup inside our dilution fridge and hanging from a mass-spring system. **(d)** Picture of the fiber holder and ring resonator mounted on the piezo positioners.

we require the minimum value measured through a full FSR scan to be higher than 90% of the base value B. This requires that the transmission through the fiber stays relatively stable throughout a full FSR scan. A free fiber can be brought back into coupling if the minimum value is lower than 80% of the base value B. By moving the ring resonator up and down we can now cycle between coupling and no coupling. Every time we are coupling we also measure the average value over a full FSR scan. If the average value is bigger than $0.93B$ we assume that there is no or little over-coupling and bulk absorption, meaning the fiber is close to the edge of the optical resonator. In this case we will move the fiber towards the center of the resonator to avoid drifting over the edge. If the average value is lower than $0.93B$ we assume that we have overcoupling or bulk absorption and move the fiber towards the edge of the resonator to keep it within the desired coupling region. Note that these movement actions are decided on while we have coupling, but we only act on these decisions once the resonator has been moved out of coupling to avoid strain on the fiber. We repeat this cycle throughout the entire cooldown. Every time we have moved out of coupling the base value is redefined as the average transmission over a full FSR scan. This is done to account for slow changes in transmission through the entire experimental system during the cooldown. We can limit the algorithm to 5 cycles per hour and still counteract any alignment changes caused by thermal contraction. This further

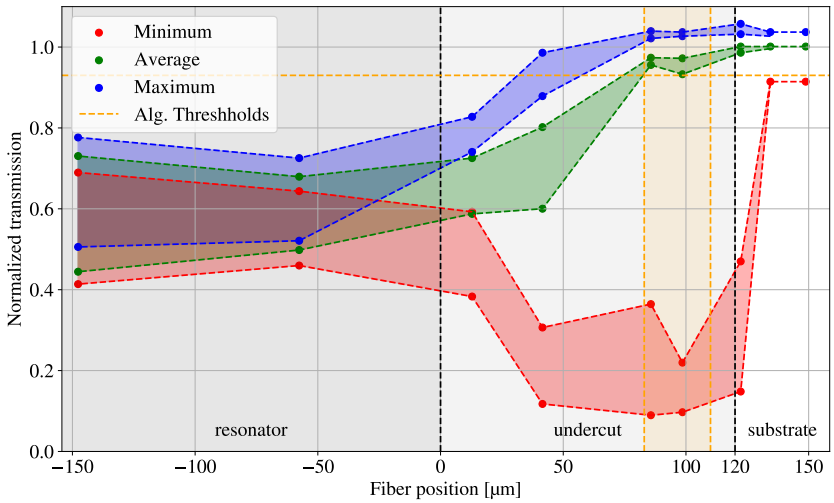

Figure 4.6: Key spectrum parameters depending on fiber position. Minimum, average and maximum transmission depending on the position of the fiber. The range for each parameter stems from uncertainty in the vertical position of the fiber. The threshold value deciding on the horizontal movement direction of the fiber as well as the resulting explored region is shown in yellow. Adapted from [83].

reduces the risk of a broken fiber and minimizes wear of the stepper motors. Generally, we have found that taking 5 steps with the motor per movement action works well for our system. We have successfully used this method to keep optical coupling for 5 cooldowns and recorded the steps taken by the motors as shown in figure 4.7. Movement of the fiber along the horizontal x-axis is generally kept to a small range throughout the cooldown. We were able to significantly reduce the range of movement along the x-axis by multiple improvements. We improved the reliability and step reproducibility of the motor by adjusting the supplied voltage and repetition rate of the motor driver depending on the temperature. Initially, the control algorithm also relied on maxima measured throughout a full FSR Scan. Instead, using the measured average of such a scan made the algorithm much more robust to deal with different scan parameters and small changes in the vertical position of the optical resonator. Optimizing the initial position of the fiber further minimized the initial movement to find the desired coupling region.

The largest amount of movement needed to keep coupling happens along the vertical z-axis. We adjust the recorded z-axis data for unequal step sizes due to gravity by

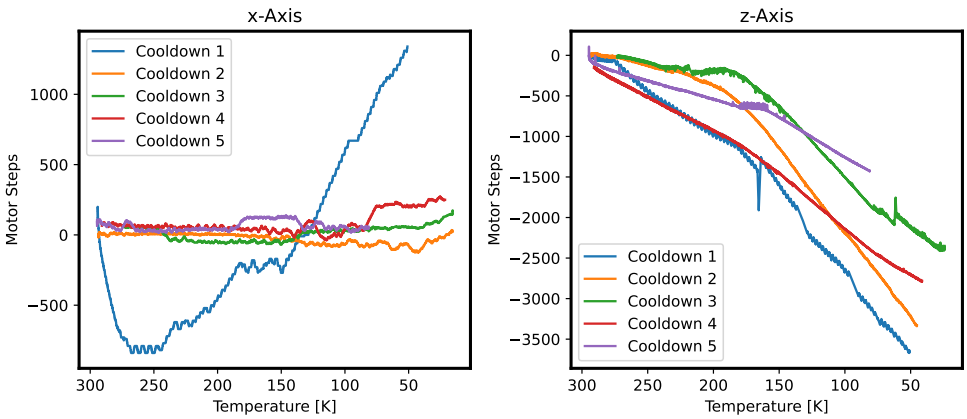

Figure 4.7: Motor steps to keep optical coupling during 5 cooldowns. x-Axis shows the horizontal movement of the fiber. Positive motor steps move the fiber towards the center of the optical resonator. z-Axis shows the vertical movement of the optical ring resonator. Positive motor steps move the optical ring resonator upwards.

performing a linear fit to the z-axis movement over the first hour and then subtracting this fit from all data points. This time frame is used as there is a negligible amount of temperature change at our system during the first hour after the pulse tube is switched on. The adjusted data shows that the optical ring resonator needs to be continuously moved downwards to adjust for alignment changes due to mismatched thermal expansion coefficients. This movement agrees with the observation that the fiber slipped underneath the undercut of the optical resonator during early cooldown attempts without stepper motors. We attribute the sharp features of cooldown 1 and 3 to a sudden degradation in motor performance, that was either resolved by increasing the driving voltage or rectified itself after repeated driving attempts.

We can find a rough estimate of distance corresponding to the steps taken by the motors by assuming the step size at room temperature to be 0.5 μm. The piezo-electric effect in the ceramics used within the motors generally decreases with decreasing temperature. At 4 Kelvin such a piezo material only expands by a fifth of the expansion at room temperature for the same applied voltage. Assuming a linear relation for this effect, we can estimate that an average of 2000 steps taken throughout a cooldown correspond to about 600 μm of distance traveled, which is well within the total travel range of the motor. Comparing the vertical size of the undercut to be about 100 μm we can conclude that we overestimate the average step size by a factor 6. This discrep-

ancy is most likely due to the rough estimate of the initial step size, the simplification of the piezo-electric response to temperature, and further temperature effects affecting the performance of the stepper motors such as changing spring tension on the slider of the motor.

4.3.3 Coupling optimization at 4 K

While the control algorithm generally keeps the optical alignment close to the desired region, it keeps the fiber away from the edge of the undercut. This is done to avoid that the fiber slips over the edge of the resonator, which would lead to a failure of the control algorithm. To achieve critical coupling to a low-order optical mode we manually adjust the alignment at 4 Kelvin. At a temperature below 20 Kelvin we stop the control algorithm and start to optimize coupling when we have reached 4 Kelvin. We first scan the laser over 1 FSR, monitor transmission and pick a mode that happens to be coupled well at the end position of the control algorithm. We optimize the optical coupling to this mode by adjusting the input polarization. We then move the sample out of and into coupling and slowly move the fiber closer to the edge of the optical resonator in between. We keep track of minimum and average of the transmission to track our progress. After a few of these cycles we once again pick the best coupled mode and adjust the input polarization to optimize optical coupling. In this way, we can find optical alignments that allow 80-90% optical coupling to an optical mode. Once this alignment is reached, we use two key indicators to determine if we couple to a low-order optical mode. We perform a small range scan over this optical mode to determine the Q-factor of the mode and check the amount of modes with a coupling of more than 10%. Generally, higher order modes have a lower Q-factor. Additionally, if the alignment is optimized to couple to a high-order mode it generally also couples well to many other modes due to the higher mode density. If both indicators suggest that we couple to a high order mode, we keep moving towards the edge as described above. Once we only couple well to only a few modes, we pick the one with the highest Q-factor and optimize input polarization. We then use single steps of both motors to optimize the alignment and achieve optical coupling above 90% as shown in figure 4.8. This optical alignment remains stable when cooling to the base temperature of our dilution fridge from 4 K to 20 mK.

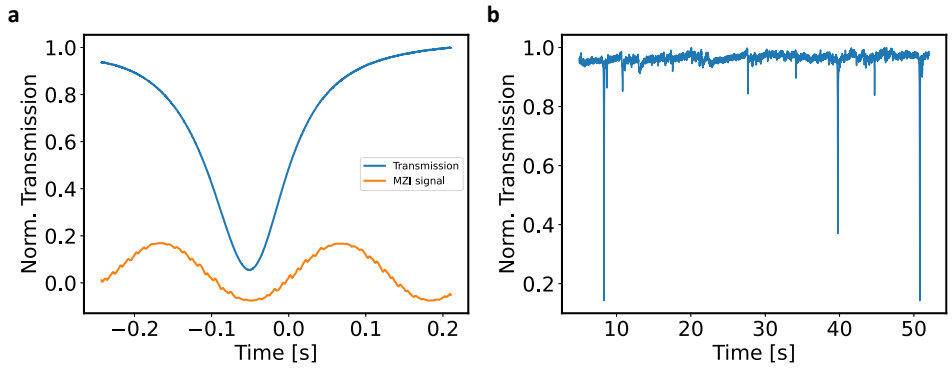

Figure 4.8: Critical coupling at 20 mK. (a) Small range scan of a mode with a coupling of 95% and Mach–Zehnder interferometer (MZI) signal to measure the Q-factor. The MZI has a fringe separation of 20.17 MHz. **(b)** Scan over one FSR after coupling to one mode has been optimized.

4.4 Conclusion

In this chapter we have presented our capabilities to reliably produce tapered optical fibers allowing for optical coupling to a wide range of devices. For an optical wedge ring resonator with a radius of 3 mm coupled to a tapered fiber detailed steps to package the assembly within a superfluid tight chamber for cooldown in a dilution cryostat have been presented. We have shown the repeated success of an algorithm that keeps the optical alignment during cooldown and demonstrated critical coupling at a temperature of 20 mK. The development of this setup has enabled optomechanical experiments with thin films of superfluid helium, as will be presented in chapter 5 and chapter 6.

4.5 Appendix

4.5.1 Details of a superfluid tight enclosure

A superfluid enclosure has to be atomically leak tight and remain that way from room temperature to mK temperatures. Superfluid helium flows relatively fast through extremely small openings due to its lack of viscosity and can therefore rapidly escape an enclosure with a small hard to detect leak. In the following I present practices that have enabled a high rate of success.

Capillary and feedthroughs

A capillary from the outside of the dilution fridge to the inside of the cell allows us to tune the thickness of the superfluid film while the fridge remains at 4 Kelvin and below. It is generally not possible to install one continuous piece of capillary reaching from the top of the fridge to the bottom of the mixing chamber. Additionally, different capillary diameters can help to maximize flow while minimizing the thermal load on the mixing chamber.

We use capillary with an inner diameter (ID) of 0.7 mm (and outer diameter (OD) of 1.1 mm) between room temperature and 4 K plate, while we decrease the ID to 0.4 mm (OD 0.7 mm) between 4 K plate and superfluid Cell. Both capillaries are made of a Copper-Nickel alloy. Capillaries with matching ID and OD can easily be joined by soldering them together. We use a scalpel to cut the capillary to the desired length. The capillary should not be deformed by applying only downwards pressure. Instead, the capillary can be carefully cut halfway and then bent open. We prepare the end of both capillaries by cleaning them with isopropanol (IPA). We then add solder on the outside around the circumference of the smaller capillary about 2 cm away from the opening. We also add solder on the outside around the circumference of the bigger capillary right at the opening. At this step, we have to be careful that no solder enters the inside of the capillary as capillary forces suck the liquid solder into the tube and close it up. If this happens a small part of the capillary can be cut and the step can be repeated. The smaller capillary can then be inserted into the bigger capillary until the two prepared solder points meet as shown in figure 4.9. The solder can then be connected with a soldering iron by a moving the soldering iron from the bigger capillary towards the smaller capillary and repeating this around the circumference.

Figure 4.9: Capillary. Left: Thermalization of the capillary. Middle: Joining of two capillaries before soldering them together. Right: Joining of two capillaries after soldering them together.

After this step we check the flow through the connection, by applying a small positive pressure (e.g. by a Nitrogen/Helium gas bottle) on one side of the capillary and holding the other (free) side into a shallow beaker with IPA. We should see a continuous stream of bubbles coming out of the capillary. Additionally, the joint should be leak checked once the entire system is assembled. Two pieces of the same capillary can be joined in the same way using a bigger piece of capillary with a length of about 5 cm.

To feed the capillary into the superfluid cell a larger rigid stainless steel tube is welded to a hole in one of the cells lids. The capillary is then fed through the tube and soldered in place.

Feedthroughs for two fibers or up to 4 thin wires can be made by drilling a hole with a diameter of 1 mm into the cell. After feeding fibers or wires through the hole can be closed with Stycast[3]. The surface with the hole should be placed horizontally such that a drop of Stycast placed on top of the hole can flow into the hole and completely cover it. At the end of the process Stycast should be visible at the other end of the hole. The feedthrough can be reused by cutting the old fibers or wires, heating the surface with a heat gun and pushing the Stycast out with a matching drill bit.

[3]Loctite Stycast 2850 FT with Catalyst 24LV

Indium seal

The lids for the superfluid tight enclosure can not be sealed with a simple rubber O-ring like is common at room temperature, and even Viton rings that are often used for cryogenic applications don't provide a perfect seal. Instead we use indium wire [85], which is a soft metal that can be pressed between two metal surfaces. We prepare the surface of the lid and cell by scrapping off old indium with a hard plastic scraper and IPA. We use an indium wire with a diameter of 1.5-2 mm that can be made to order at our fine mechanical department. The lids feature an extrusion on the inside that we can tightly lay the indium wire around. At the meeting point of the two ends of the indium wire we use a scalpel to cut both ends of the indium wire with a sharp angle, such that the cut surfaces can be connected to form one joined loop. We then place the lid onto the cell and make sure the indium wire did not slip out of position. We then tighten the screws slowly and in a circular pattern to distribute the indium evenly. We repeat this until the force required rises sharply. Since indium is slightly toxic when ingested one should wear gloves while handling it.

Over multiple runs old indium may build up and can not be easily removed mechanically, which can lead to leaks. To clean a surface of indium remains, one can either polish the surface and remove a small amount of the underlying material or place the surface in hydrochloric acid under a chemical hood for a few hours to dissolve the indium.

Acknowledgments

I thank Harmen van der Meer and Robin Schrama from the fine mechanical department (FMD) for their contribution to the fabrication of the optical setup, the superfluid cell and the capillary. I thank Geert Timmerman for his contribution to building the fiber taper setup and characterizing the coupling regions of the wedge resonator.

4.